

Finding the Missing Baryons Using CMB as a Backlight

Shirley Ho*

*Department of Astrophysical Sciences,
Princeton University, Princeton, NJ 08544*

&

Lawrence Berkeley National Laboratory, Berkeley, CA 94704

Simon DeDeo

*Kavli Institute for Cosmological Physics,
University of Chicago, Chicago, IL 60637, USA*

&

*Institute for the Physics and Mathematics of the Universe,
University of Tokyo, Kashiwanoha 5-1-5,
Kashiwa-shi, Chiba 277-8582, Japan*

David N. Spergel

Department of Astrophysical Sciences, Princeton University, Princeton, NJ 08544

(Dated: November 7, 2018)

We present a new method for detecting the missing baryons by generating a template for the kinematic Sunyaev-Zel'dovich effect. The template is computed from the product of a reconstructed velocity field with a galaxy field; we find that the combination of a galaxy redshift survey such as SDSS and a CMB survey such as ACT and PLANCK can detect the kSZ, and thus the ionized gas, at significant signal-to-noise. Unlike other techniques that look for hot gas or metals, this approach directly detects the electrons in the IGM through their signature on the CMB. The estimated signal-to-noise for detecting the galaxy-momentum kSZ cross-correlation is 4, 9, and 12 for ACT (with survey area of 2000 deg²) with SDSS-DR4, SDSS3 and ADEPT respectively. The estimated signal-to-noise for PLANCK with SDSS-DR4, SDSS3 and ADEPT is 11, 23, and 32. Our method provides a new mean for determining properties of the ionized gas in the Universe. We provide galaxy momentum templates constructed from Sloan Digital Sky Survey online at our website at <http://www.astro.princeton.edu/~shirley/SZ/SZ.html>. The predicted correlation coefficients are provided along with the momentum maps. One can download the momentum templates and cross-correlate directly with CMB maps from ACT and PLANCK to detect the missing baryons.

Where are the baryons? Astronomers can measure the baryon abundance three minutes after the big bang using Deuterium [1], 300,000 years after the big bang using the angular power spectrum of the Cosmic Microwave Background [2], and at redshift three using the Lyman- α forest [3]. However, today, most of the baryons are missing [4]. Too hot to show up in Lyman- α absorption studies, too cool to find in spectral distortions of the cosmic microwave background, and hidden in large-scale structures of the cosmic web of too low a density to appear in the X-ray, finding this missing matter is one of the open challenges in cosmology.

The baryons within clusters – shock heated during virialization of the structure – have been the subject of extensive study with X-ray telescopes [5, 6, 7]. However, as X-ray emission strength is proportional to the square of electron density, these studies can only detect baryons in the very center of clusters. There have been numerous attempts to make X-ray observations of the filamentary gas [8], but filamentary gas seems to elude X-ray detection.

Baryons within clusters are now being detected at significant confidence levels through their distortion of the primordial black-body spectrum, both in observations targeted towards known clusters [9], in cross-correlation with the WMAP data [10, 11, 12], and now in blind surveys as the latest detectors come online [13]. This effect, known as thermal Sunyaev-Zel'dovich (hereafter tSZ, [14]), is, at the arcminute scales to be probed by current and upcoming experiments such as the *Atacama Cosmology Telescope* (ACT), the *South Pole Telescope* (SPT) and the *Planck* satellite, the strongest signal (in two-point correlation) on the microwave sky. Measurements of the tSZ effect can detect baryons in clusters. The tSZ, however, depends for its strength on both the density and the temperature of the gas, and so an experiment that may detect the gas at the center of a cluster, where temperatures can reach over 10⁷ K, will be unable to find at all the gas associated with the far less dense, and far colder, material that lies in the filaments of the cosmic web [15].

Even when a survey reaches sensitivities of 2 $\mu\text{K arcmin}^{-2}$, identifiable tSZ sources are all objects with mass greater than $2 \times 10^{14} M_{\odot}$ [16], and most of the contribution to the power spectrum comes from virialized gas in groups just below the detection mass [17].

*Electronic address: cwho@lbl.gov

The kinetic Sunyaev-Zel'dovich effect [14, hereafter kSZ], in contrast to the tSZ, depends not on the thermal motions of the gas, but rather on the bulk velocity of the structures the gas inhabits. In particular, the flows of matter toward overdensities Doppler-shift CMB photons to produce anisotropies. The fractional change in temperature due to kSZ, $\Theta = \Delta T/T_{cmb}$, is

$$\Theta(\hat{n}) = - \int_0^{\eta_0} d\eta g(\eta) \mathbf{n} \cdot \mathbf{p}(\hat{n}\eta, \eta), \quad (1)$$

where \mathbf{n} is the unit vector pointing away from the observer and the momentum field, p , is defined as

$$\mathbf{p}(\hat{n}\eta, \eta) = [1 + \delta_b(\hat{n}\eta)] \mathbf{v}_b(\hat{n}\eta, \eta), \quad (2)$$

and δ_b is the baryon overdensity, and the \mathbf{v}_b is the baryon velocity. The visibility function g is defined as

$$g(\eta) = x_e \tau_H (1+z)^2 e^{-\tau(z)}, \quad (3)$$

and x_e is the ionization fraction, τ_H is the Thompson-scattering optical depth to the Hubble distance today; τ , in the reionized epoch, is

$$\tau(z) = \frac{2}{3} \frac{\tau_H}{\Omega_m} [\sqrt{1 - \Omega_m + \Omega_m(1+z)^3} - 1] \quad (4)$$

and, finally, η is the comoving distance defined in units of Hubble distance:

$$\eta(z) = \int_0^z \frac{H_0}{H(z')} dz'. \quad (5)$$

Baryons in the cosmic web have sufficient velocity and column density to produce a detectable kSZ signal [18]. Indeed, at arcminute scales, the kSZ is expected to be the strongest anisotropy after subtraction of the tSZ using frequency information [19]. Here we demonstrate a new method for extracting the kSZ that is not subject to the systematics one might expect when trying to see it in the two-point CMB auto-correlation.

In particular, we consider the idea of cross-correlating the CMB sky with a kSZ template constructed by projecting down the line-of-sight momentum field of large scale structure. This momentum field is reconstructed from the inferred three-dimensional dark matter distribution. We construct such a template from the latest large scale structure data, and make it available to the scientific community.

To generate the momentum field we require knowledge of the velocity field. We can rely upon the linearity of the large-scale velocity field, $\mathbf{v}(\mathbf{k})$, which is related to the density field via the continuity equation,

$$\mathbf{v}(\mathbf{k}) = i \frac{d \ln G}{d \ln a} \frac{a H \delta_m(\mathbf{k}) \mathbf{k}}{k^2}, \quad (6)$$

where a is the scale factor, G is the growth factor at late times (proportional to a in the matter dominated regime), δ_m is the matter density fluctuation field and k is

the comoving wave number. This is strictly valid only on larger scales where material remains in the linear regime; we shall determine how well it holds in approximation and on different scales in the following section.

The temperature increment for a particular velocity estimate depends on both the cosmological parameters through Eq. 6, and on the gas column density and thus, in conjunction with other observations that can constrain cosmological parameters, can unambiguously detect the missing baryons in the large, low-density filaments that have undetectable tSZ.

There are two major advantages to this method over others that have been proposed. The first is that we expect the sign of the line-of-sight velocity to be uncorrelated with many of the standard systematics, such as insufficiently subtracted tSZ, galactic foregrounds, and detector and telescope noise.

Secondly, our method makes near-maximal use of the information available in a potential cross-correlation. Previous studies of constraining dark energy parameters by using kSZ information in cross-correlation with a CMB signal have “thrown out” some of the signal, dropping the phase information that determines the sign of the kSZ signal, and information about where velocity flows are most likely to be found.

The idea of using peculiar velocity flows in a galaxy survey to do cosmology has been studied in past decades, most notably by the use of redshift and luminosity distance indicators for very nearby ($z < 0.1$) objects [20]. However, the method we propose here has only become technically feasible in recent years with the combination of large scale redshift surveys and the current and upcoming arcminute scale CMB experiment, and the issues and questions we must confront are very different.

Our paper has four parts: the reconstruction of the velocity field (Sec. I), the determination of the cross-correlation coefficients (Sec. II), signal-to-noise estimates for current and forthcoming surveys (Sec. III) and the template construction (Sec. IV) using actual large scale structure data from SDSS.

I. VELOCITY FIELD RECONSTRUCTION

We first detail our method of velocity reconstruction, which provides us with the velocity field that is accurate in large range of scales which are relevant to the structures that harbor most of the gas in the Universe. We also validate our reconstruction method via a N-body simulation.

A. Theory

The Universe provides us with the redshift space overdensity field, and there are many ways we can construct a real space density (see, *e.g.*, [21]). We take here the simplest approach, since the scales we are interested in

are not strongly affected by non-linear effects – fingers of God, for example, occur on cluster scales, whereas the velocity field has most power on scales larger than 10 Mpc. We directly transform the redshift density field into a real space density field using the Friedman equation (with WMAP5 parameters), and embed the real space density field in a box. We compute the overdensity field in real space, convert it to Fourier space, and use the transformation described by Eq. 6 to determine the velocity field. We then convert this field back into real space, and use this representation to study the properties of cosmological velocity flows.

Our method falls into six steps.

1. Transform the redshift space overdensity field to real space overdensity field.
2. Fourier transform the overdensity field.
3. Wiener-filter (as discussed below) the map given our knowledge of noise from Poisson statistics and non-linearities.
4. Apply Eq. 6 to compute $\mathbf{v}(k)$.
5. Inverse Fourier transform $\mathbf{v}(k)$ to find the real space velocities.
6. Transform the real space velocities back to redshift space, and find the momentum field by taking the product with a density survey (which may or may not be the same as the survey used to determine the velocities.)

While this method sounds simple, its error properties can be hard to estimate. In particular, even if observational noise in the density field is uncorrelated (*e.g.*, in the case of Poisson noise alone), the noise in the velocity field will be correlated from point to point. Formally, this can be seen by noting that the Fourier transform of $1/k$ is proportional to $1/r^2$, and so in real space computing the velocity field corresponds to convolving with the gravitational force kernel. The induced statistical errors remain Gaussian – but their spatial correlation is no longer a delta function.

It is also important to recognize that points near the edges of the survey will have errors from our lack of knowledge of what lies beyond the survey volume. Intuitively, one can imagine the possibility of a “great attractor” lying just outside the boundary [22, 23], changing the velocity field radically from the estimate produced by using only the observed material. Developing mathematical techniques to determine the influence of these errors on the momentum field is difficult. We side-step the problem in this section by using an N-body simulation, where we have knowledge of the true velocity field.

B. Simulation

We check the validity of our reconstruction method with simulations. We first simulate a galaxy field and

then implement our method of computing the velocity field. We then compare our recovered velocity field to the true velocity field in the simulation and investigate how well the reconstruction has worked.

Our N-body simulation uses WMAP 5-year parameters, has volume $256^3 h^{-1}$ Mpc and contains 256^3 particles. The linear CDM power spectrum was generated using code from the GRAFIC2 [61] package [24]. GRAFIC2 was then used to generate the initial particle conditions, with the modification that the Hanning filter was not used because it suppresses power on small scales [25]. Simulations were carried out using the TPM [62] code [26] with a 256^3 mesh and a spline softening length of $20.35 h^{-1}$ kpc. The initial domain decomposition parameters in the TPM code were $A = 1.9$ and $B = 8.0$ (TPM was modified slightly so that there was no lower limit to B when it is reduced at later times, which improves the tracking of low mass halos; for details on these parameters see [26]).

We take this simulation and find its halos using a friends-of-friends (FOF) algorithm. After we identify the halos, we use the Halo Occupation Distribution (HOD) from Bootes field [27] to populate the halos with galaxies. The galaxies were selected in the Bootes field by enforcing uniform comoving number density of $\bar{n} = 10^{-3}(\text{Mpc}/h)^{-3}$. We then only take these galaxies and compute the overdensity field. This allows us to assess the effects of incomplete sampling of the dark matter field by the galaxies.

To quantify the accuracy of the construction, we define a velocity reconstruction coefficient, $r(k)$, as:

$$r(k) = \frac{\langle \mathbf{v}^{\text{recon}}(k) * \mathbf{v}^{\text{sim}}(k) \rangle}{\langle \mathbf{v}^{\text{recon}}(k) * \mathbf{v}^{\text{recon}}(k) \rangle}, \quad (7)$$

where $\mathbf{v}^{\text{recon}}(k)$ are the reconstructed velocities, and \mathbf{v}^{sim} those found by the simulation itself. This is a simple way for us to gauge how good we can reconstruct velocities in the presence of both Poisson noise (from incomplete sampling of the dark matter field by galaxies) and break-downs of Eq. 6 due to non-linear evolution.

We apply a Wiener filter to the density field before we reconstruct our velocity field, defined as follows:

$$W_v(k) = \frac{b^2 r^2(k) P(k)}{b^2 P(k) + \frac{1}{\bar{n}}}, \quad (8)$$

where $P(k)$ is the dark matter power spectrum, b is a (possibly weighted) average bias for the survey, and \bar{n} is the number density of the survey.

By comparing the top and bottom panels of Fig. 1, one can see the effect of this filter on the reconstruction; while small scale power in the velocity field is filtered out, the large scale velocities are traced reasonably well. The Wiener filter for generating the density field is simpler, since there is no additional “reconstruction error” as there is for the velocity:

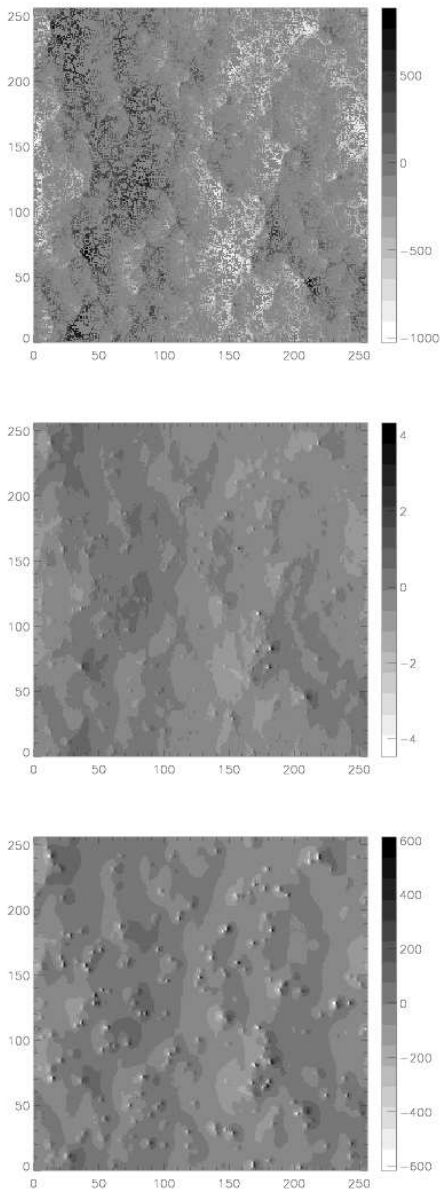


FIG. 1: The top panel shows velocity in z -direction for a slice in our simulation. The middle panel shows the reconstructed velocities of one slice of the simulation when we use all the dark matter particles in the box. The bottom panel shows the reconstructed velocities of the same slice with Wiener filtering. The velocities (only in z -direction) are pointing left and right of the map in both panel.

$$W_{\text{gal}}(k) = \frac{b^2 P(k)}{b^2 P(k) + \frac{1}{n}}, \quad (9)$$

We have two main sources of noise: an inability to determine non-linear velocities fields, and Poisson noise from galaxies. The effect of the latter can be seen in the bottom two panels of Fig. 1; the middle panel uses all

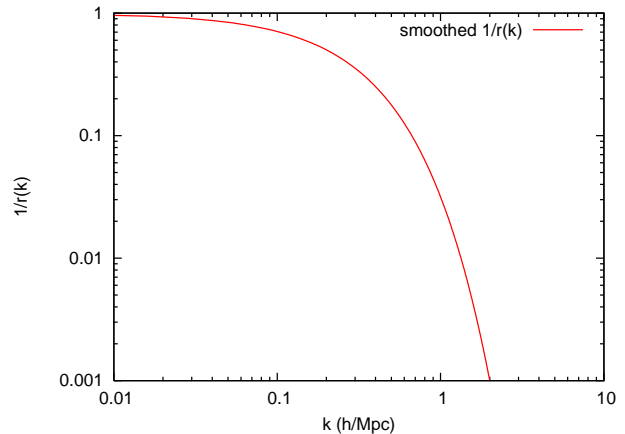


FIG. 2: Smoothed correlation coefficients ($1/r(k)$) between the reconstructed velocities and the real velocities are shown here. At small k , the limited size of the simulation box provides us with insufficient information to reconstruct extremely large scale velocities – thus the drop off at small k . At large k , where non-linear effects kick in, the linear theory we apply to reconstruct velocities is not valid anymore. We however smoothed out the small k drop off, since this is an artifact of the limited simulation box size. We smoothed out the correlation coefficients at all scale so that we can apply a smooth $r(k)$. However, for a large range of scales we have nearly perfect reconstruction.

the particles in the simulation and so is sensitive to non-linear breakdowns of Eq. 6; the bottom panel uses only ‘galaxies’ to reconstruct the velocities, thus is sensitive to both the non-linear breakdowns and also the Poisson noise from galaxies.

As we can see in a plot of $r(k)$ in Fig. 2, the velocity field reconstructed from the galaxy density field agrees well with both the velocity field reconstructed from the matter field and with the full velocity field of the simulation. There is a significant range of k in the linear regime that is well-reconstructed, while the correlation drops off at non-linear regime.

The studies of this section thus suggest that velocity reconstruction is a viable method even in the presence of the levels of noise we might expect in a contemporary large-scale structure survey. We now turn our attention to making an analytic estimate of the k SZ signal.

II. ESTIMATING THE KSZ SIGNAL IN ℓ -SPACE

Having validated our reconstruction method, we now turn our attention to predicting the dependence, on cosmological parameters, of the cross-correlation between a projected momentum field and the CMB.

A. Theory

The velocity field in the linear regime is a pure gradient field: the direction of the velocity is aligned with the direction of its k -mode. Combining Eqs. 2 and 3 in the Limber approximation, then, we can see that the source of the signal will be primarily from a modulation of this velocity field by the density field. This “second-order” nature of the kSZ was realized early on [28].

There is also the possibility of modulating the velocity field by the visibility function: the so called “velocity-Doppler” effect that can be significant on large scales. However this signal is drawn primarily from redshifts around reionization where the derivative of the ionization fraction is large [29]; it does not correlate with a low-redshift survey.

To estimate the momentum-kSZ cross-correlation signal, we must first make assumptions about how well our various observables trace the underlying dark matter and baryon fields. We take, as reasonable *Ansätze* for the relationship between baryon, dark matter and galaxy overdensities:

$$\delta_b(k) = f(k)\delta_m(k) \quad (10)$$

and

$$\delta_{\text{gal}}(k) = b(k, z)\delta_m(k), \quad (11)$$

where $f(k)$ describes the difference in clustering power between baryons and dark matter – we take the functional form of [30] – $b(k, z)$ is the scale and redshift dependent bias of galaxy overdensity field, and $\delta_m(k)$ is the non-linear cold dark matter overdensity field. We take \mathbf{v}_{gal} , our reconstructed velocity field discussed in the previous section, to be

$$\mathbf{v}_{\text{gal}}(\mathbf{k}) = i \frac{d \ln G}{d \ln a} \frac{aH \delta_{\text{gal}}(\mathbf{k}) \mathbf{k}}{k^2}, \quad (12)$$

where, note, we do not divide out by the bias; this allows us to keep a handle on how bias estimates will affect our final result, and we similarly use $f(k)\delta_{\text{gal}}$ as our estimate of baryon overdensities.

Once we apply the Wiener filters of Eqs. 8 and 9 to our estimates of the baryon velocity field, Eq. 12, and the baryon density field, we may Fourier transform into real space and project down to produce the reconstructed, projected momentum field, which we call Q .

We can then ask: how well does Q correlate with Θ ? We here follow and elaborate on the analysis of Ref. [31]. We know that \mathbf{v}_{gal} and \mathbf{v}_b are imperfect correlates, and assume that $r(k)$, defined in Eq. 7, captures all of these effects; this amounts to assuming that baryon velocities are governed entirely by gravity and so track the cold dark matter – a reasonable assumption on the scales we consider.

We further assume that the effects of Poisson noise, non-linear velocity fields, and non-gravitational interactions are not correlated with the linear field, and that

differences between dark matter and baryon flows on the relevant scales are negligible, so we may write,

$$\begin{aligned} \langle v_b(\mathbf{k})v_{\text{gal}}(\mathbf{k}') \rangle &= (2\pi)^3 \delta_D(\mathbf{k} - \mathbf{k}') \\ &\times b(k, z)r(k) \left(\frac{d \ln G}{d \ln a} \frac{aH}{k} \right)^2 P(k), \end{aligned}$$

where $P(k)$ is the non-linear cold dark matter power spectrum; note that the correlation here depends also on bias.

We write the angular power spectrum of the cross-correlation as

$$C_l^{\mathbf{Q}\Theta} = \frac{\pi^2}{2l^5} \int d\eta \eta^3 g(\eta) N(\eta) \left(\frac{\dot{G}(\eta)}{G(\eta)} \right)^2 I_{\mathbf{Q}\Theta}(l/\eta), \quad (13)$$

where η is comoving distance in units of Hubble distance as defined in Eq.5, $G(\eta)$ is the growth factor at η , and overdots are with respect to η . $I_{\mathbf{Q}\Theta}$ is the cross-power spectrum of the vorticity of the momentum field, which we can, after manipulation, write as

$$\begin{aligned} I_{\mathbf{Q}\Theta}(k, z) &= \int_0^\infty dy_1 \int_{-1}^1 d\mu \frac{(1 - \mu^2)k^6}{4\pi^4} \\ &[b(k')f(k')P(k')W_{\text{gal}}(k') \\ &b(k'')r(k'')P(k'')W_v(k'') - \\ &\frac{y_1^2}{y_2^2} b(k')r(k')P(k')W_{\text{gal}}(k') \\ &b(k'')f(k'')P(k'')W_v(k'')], \quad (14) \end{aligned}$$

$k' = ky_1$, $k'' = ky_2$ and y_2 is equal to $\sqrt{1 - 2\mu y_1 + y_1^2}$.

To compute the signal-to-noise, we will also need the auto-correlation of the template,

$$C_l^{\mathbf{Q}\mathbf{Q}} = \frac{\pi^2}{2l^5} \int d\eta \eta^3 N(\eta)^2 \left(\frac{\dot{G}(\eta)}{G(\eta)} \right)^2 I_{\mathbf{Q}\mathbf{Q}}(l/\eta). \quad (15)$$

Since we Wiener filter both the density field and the velocity field in the construction of the template \mathbf{Q} , $I_{\mathbf{Q}\mathbf{Q}}$ is not identical to $I_{\mathbf{Q}\Theta}$; we find

$$\begin{aligned} I_{\mathbf{Q}\mathbf{Q}}(k, z) &= \int_0^\infty dy_1 \int_{-1}^1 d\mu \frac{(1 - \mu^2)k^6}{4\pi^4} \\ &[b^2(k')P'(k')W_{\text{gal}}^2(k') \\ &b^2(k'')P'(k'')W_v^2(k'') - \\ &\frac{y_1^2}{y_2^2} b^2(k')P'(k')W_{\text{gal}}(k')W_v(k') \\ &b^2(k'')P'(k'')W_{\text{gal}}(k'')W_v(k'')] \quad (16) \end{aligned}$$

We have here defined $P'(k)$ as $P'(k) + 1/b^2(k)\bar{n}$.

The “science product” consists both of a template Q , defined in this section, and an estimate, $C_l^{\mathbf{Q}\Theta, \text{analytic}}$, of its cross-correlation amplitude with the CMB for a set of fiducial choices for the cosmological and galaxy survey

parameters. The ratio, R of this estimate to that actually measured with an experiment is

$$R = \frac{C_l^{\mathbf{Q}\Theta, \text{observed}}}{C_l^{\mathbf{Q}\Theta, \text{analytic}}} \propto b_{\text{eff}}^2 g_{\text{eff}} \quad (17)$$

where b_{eff} is an “effective” averaged bias, weighted by the various kernels $g(\eta)$ and $N(\eta)$, g_{eff} is the effective averaged visibility function within the survey volume that has been weighted similarly as the bias. In the case that the fiducial parameters chosen are the true ones, R is unity.

B. Validating Estimates

Since this is the first time this method has been constructed and applied, we check the validity of our calculation for $C_l^{\mathbf{Q}\Theta}$ through numerical simulations, in the following fashion:

1. We produce the “real” kSZ sky, Θ , with an N-body dark matter particles simulation box (as described earlier in Sec. IB) from $z = 0.428$ and assuming that the ionized gas traces the dark matter.
2. We produce the template, Q , with FOF (friends-of-friends) halos found from the same N-body and then use an HOD (from Ref. [27]) to populate the halos with their galaxies.
3. We project these two fields, and take their cross-correlation to find $C_l^{\mathbf{Q}\Theta, \text{sim}}$.

Note that the highly limited red-shift range of our simulations means that we will not reproduce an entire kSZ sky – only that produced by baryons in a very limited range.

Fig. 3 compares these two quantities; we find that at scales where there are a sufficient number of modes in the N-body to do our reconstruction reliably, the analytic calculations perform well and without appreciable bias.

Given the expected signal-to-noise of upcoming measurements, then, the precision of our analytic formula for $I_{\mathbf{Q}\Theta}$ are more than sufficient for accurate determination of gas parameters.

III. ESTIMATING SIGNAL-TO-NOISE FOR THE KSZ CROSS-CORRELATION SIGNAL

In this section, we evaluate whether current and upcoming surveys are capable of using the method developed in this paper to detect the kSZ-galaxy momentum template cross-correlation. Our method requires two very different types of observations: a sensitive high resolution CMB map (e.g., PLANCK, ACT or SPT) and a large-volume spectroscopic survey (e.g., SDSS, SDSS3,

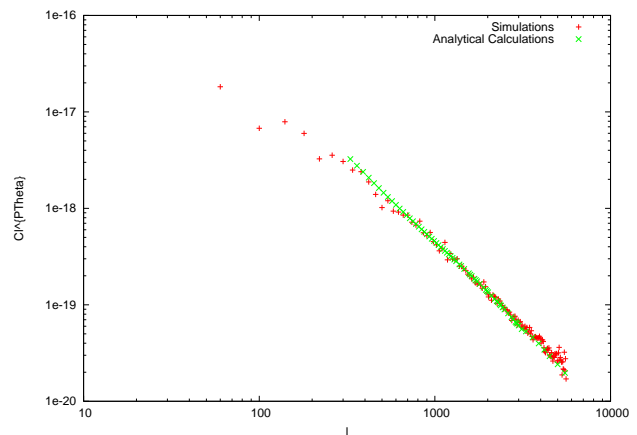


FIG. 3: We show the validity of our equations via comparison between the expected cross-correlation coefficient $C_l^{\mathbf{Q}\Theta, \text{analytic}}$ and the calculated cross-correlation coefficient from simulations $C_l^{\mathbf{Q}\Theta, \text{sim}}$.

ADEPT). We estimate the expected signal/noise in the combined maps by computing:

$$\left(\frac{S}{N}\right)^2 = f_{\text{sky}} \sum_l (2l+1) \frac{(C_l^{\mathbf{Q}\Theta})^2}{C_l^{\mathbf{Q}\mathbf{Q}}(C_l^{\text{CMB}} + C_l^{\text{DET}})},$$

where f_{sky} is the fraction of sky that is covered by both the spectroscopic survey and the high resolution CMB survey. $C_l^{\mathbf{Q}\Theta}$ is as described in Eq.13, while $C_l^{\mathbf{Q}\mathbf{Q}}$ is simply the 2-point correlation function of \mathbf{Q} (the momentum field) with its noise. From the CMB side, we have C_l^{CMB} which is the CMB temperature anisotropies (which is noise here), and C_l^{DET} which is the detector noise from the CMB experiment.

We consider the following two CMB experiments specifically:

1. Atacama Cosmology Telescope (hereafter ACT, see [63] for further information): we assume a θ_{FWHM} of $1.4'$ and a noise of $26 \mu\text{K arcmin}^{-2}$ with a survey area of 2000 deg^2 based on a straw-man proposal.
2. PLANCK (see [64] for further information): we assume a θ_{FWHM} of $7.1'$ and a noise level of $302 \mu\text{K arcmin}^{-2}$ for 75% of the sky, since galactic foregrounds may prove to be hard to subtract from parts of the maps.

For large scale structure surveys, we consider two current surveys and a proposed mission concept:

1. Sloan Digital Sky Survey (hereafter SDSS): we use the SDSS DR4 VAGC LSS sample [32] (which will be further described in Sec. IV). The bias of the main galaxy sample is found to be ~ 1.2 if we assume linear bias (see Ref. [21]). For the purpose of signal-to-noise analysis, it is sufficient to assume

S/N	ACT (2000 deg ²)	PLANCK
SDSS-DR4	4.1	11.2
SDSS3	8.5	22.5
ADEPT	12.2	32.2

TABLE I: The signal-to-noise ratio for the detection of gas-momentum-kSZ correlation for different combinations of current and upcoming experiments.

linear bias, but we will discuss the effects of bias later in Sec. V. The bias of the spectroscopic LRGs is found to be ~ 2 (based on the powerspectrum analysis done in Ref. [33]). We include bias as a free parameter throughout the theoretical calculation, with one exception. We only employ bias from other analysis when we generate filter functions (W_{gal} and W_v) as defined in Sec. IB.

2. Sloan Digital Sky Survey 3 (hereafter SDSS3, see [65] for further information): We assume the availability of 10^6 spectroscopic Luminous Red Galaxies over a quarter of the sky in the redshift range of $0.2 - 0.6$. Since SDSS3 plans to spectroscopically observe all of the photometric LRGs in SDSS, we use the redshift distribution and bias ($b \sim 2$) determined for the photometric LRGs in SDSS as described in Ref. [34].
3. Advanced Dark Energy Physics Telescope (hereafter ADEPT, see [66] for further information): we assume the availability of 10^8 galaxies over 28600 deg^2 from $1 < z < 2$. We assume a bias of 1.5 and a uniform distribution in comoving volume from $1 < z < 2$ here. Since these galaxies are Lyman-alpha emitters, we take the bias from studies by Ref. [35] which suggests a bias of ~ 1.5 .

For the S/N calculation, we also assume an ionization fraction of 1 ($x_e = 1$) and full hydrogen ionization.

IV. TEMPLATES

Finally, we illustrate our method by constructing a galaxy momentum template from the Sloan Digital Sky Survey. This template is a prediction for the ACT and PLANCK experimental specifications and this section demonstrates how to develop templates for other surveys.

A. Data from Sloan Digital Sky Survey

The Sloan Digital Sky Survey has acquired *ugriz* CCD images of 10^4 deg^2 of the high-latitude sky [36]. A dedicated 2.5m telescope [37, 38] at Apache Point Observatory images the sky in photometric conditions [39] in five bands [40, 41] using a drift-scanning, mosaic CCD camera [37]. All the data processing are done by completely

automated pipelines, including astrometry, source identification, photometry [42, 43], calibration [44, 45], spectroscopic target selection [46, 47, 48], and spectroscopic fiber placement [49]. The SDSS is well underway, and has produced seven major releases [50, 51, 52, 53, 54, 55, 56].

In this paper, we utilize mainly the SDSS DR4 VAGC ([32]) sample and also the SDSS spectroscopic Luminous Red Galaxies (hereafter LRG, [46]), since these two samples are the largest spectroscopic samples publicly available and have near-uniform completeness over a large area of sky. The spectroscopic LRG sample [46], includes area beyond Data Release 4 (DR4). The total area coverage for this spectroscopic sample is $5154 \text{ square degrees}$, as available in the NYU Value Added Galaxy Catalog (VAGC [32]) at the time of the preparation of our project.

B. Constructing Templates

We construct the templates by the following steps:

1. We select only sky areas that are covered by survey with completeness of over 85%, so that the galaxy field nearly uniformly samples the underlying density field.
2. We compute the overdensity field and embed the survey volume in a periodic box (of size $1762^3 (h^{-1} \text{ Mpc})^3$, with cells of size $6.9^2 (h^{-1} \text{ Mpc})^2$). We assume that the region without observations is at the mean density of the universe.
3. We compute the Wiener filtered density field and also the velocity field (via our six-step reconstruction method as described in Sec. I).
4. We compute the momentum field as it is projected along line of sight and calculate the 2D momentum field that would be used to cross-correlate with the appropriate CMB field to get the $C_l^{\text{Q}\Theta}$.

We made the templates available in both ACT and various PLANCK resolutions. An update of the templates with full SDSS data-set will be made as data and time allow. The templates are made available to public on our website [67]. Their respective $C_l^{\text{Q}\Theta, \text{analytic}}$ for the templates are also available as the filtering we use in the paper affect the overall normalization of the signal. In general, it is simpler to compare the provided $C_l^{\text{Q}\Theta, \text{observed}}$ and the observed $C_l^{\text{Q}\Theta}$ when one cross-correlates the templates with the CMB sky.

The two bias and gas-dependent parameters, g_{eff} (the weighted visibility function), and b_{eff} (the weighted bias) are complicated, but slowly varying, functions of the galaxy and gas fields; we take our fiducial model (R of unity) to have constant, scale-independent bias b of 1.2 (2) for main galaxy (LRG) sample, and Ω_b of 0.0441, h of 0.71 with x_e of 1.0. For reference, we plot the 2D kSZ field made from SDSS DR4 Main galaxy template here in Fig.5.

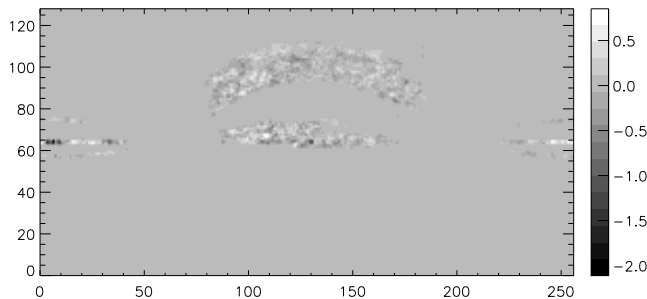


FIG. 4: Plotted is the 2D kSZ field made from SDSS DR4 Main galaxy momentum template. The template predicts both hot and cold regions (due to the fact that this is a momentum field). This implies that the template is likely to be nearly orthogonal to effects that are scale with the galaxy or the matter density (such as integrated Sachs-Wolfe effect ([57]), Rees-Sciama effect [58], tSZ, lensing, dusty galaxy emission and to the galaxy foregrounds).

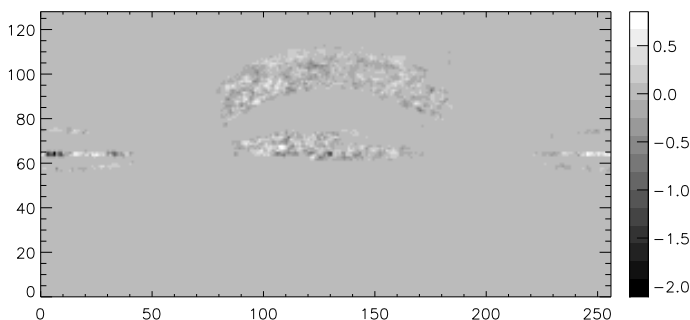


FIG. 5: The 2D kSZ template reconstructed from SDSS DR4 Value-added Galaxy Catalog (VAGC.)

V. DISCUSSION

A. Possible Caveats

Our method deals well with a number of possible interfering signals; we discuss them here.

1. **Thermal Sunyaev-Zel'dovich.** The tSZ contributes to our estimates as a noise term, since tSZ signals are uncorrelated with the velocity fields; our momentum-kSZ correlation is not biased by the presence of tSZ. In principle, we can also use multifrequency data from CMB to separate the tSZ signal from kSZ as tSZ and kSZ have different spectral signatures. We can then reduce the noise contributed from tSZ. There is in general leakage of the tSZ signal into CMB maps due to uncertainties in the detector frequency response function and due to relativistic tSZ effects (see Ref. [16]). Other contaminants that can not be picked out with frequency information, such as the Rees-Sciama (non-linear ISW) and lensing effects, are generally lower

in amplitude; they, too, contribute to the noise, but again in an unbiased fashion.

2. **Bias.** Bias is treated as redshift and scale dependent throughout our theoretical calculations. However, as the ratio between the observed and theoretical C_l are degenerate between the effective bias (b_{eff}^2) and g_{eff} , one can determine bias (with its redshift and scale dependence) but not being able to learn very much about the missing baryons.

Since one can calculate bias from the power spectrum analysis of galaxy populations, we assume that bias can be determined fully in the large scale structure survey before one uses the survey to produce the gas-momentum field of the Universe.

For simplicity in our template production we assume scale and redshift independence for bias (which is appropriate for the scale and redshift we are working with) in the production of the templates and take on values of bias which are predetermined via other efforts.

In particular we use bias determined by [21] in the construction of the filtering functions W_{gal} and W_v . In the calculation of signal-to-noise, we assume a bias for the galaxy population we (will) use to construct the template for various experiments.

3. **Dusty Galaxies.** Star forming galaxies can be very luminous at submillimeter wavelength range, as suggested by Submillimeter Common User Bolometer Array (SCUBA) and other experiments (see [59] for a review). The emission is mainly from dust around the galaxies at approximately ~ 10 K, radiating mainly at sub-mm wavelength, but can also be significant at millimeter wavelengths. Fortunately, the dusty galaxies do not correlate with the bulk flows of the Universe and thus, by the same argument presented for tSZ, do not bias the measurement of the gas-momentum-kSZ correlation.
4. **Galactic Foregrounds.** Galactic Foregrounds affect mostly the large-scale of the CMB and the galaxy observations and since they do not correlate with the large-scale velocity field, we can safely assume that it would not bias our estimator, but would at most be adding to the noise term.

We could also consider reducing the contribution of the noise from the galactic foregrounds in our cross correlation by limiting ourselves to certain multipoles where the galactic foregrounds are weak. We can gauge the effect of the galactic foregrounds by cross-correlating the momentum field with (for example) dust extinction maps [60] to find out the range of multipoles that are not affected by the galactic extinction.

B. Further applications

We can use the gas-momentum-kSZ temperature correlation to constrain not only the baryon content of selected regions of the Universe, but also the baryon profiles and evolution of its density. We give examples below to describe how in theory we can apply the gas-momentum-kSZ temperature correlation to understand gas profiles and baryon evolution over redshift:

1. Gas profiles: Assuming that we know the bias and ionization fraction of the Universe in the same region of interest, we can parameterize the electron density as a function of radius (from the center of the nearest galaxy or region under consideration) and generate the appropriate visibility functions. We can then construct momentum templates and maximize the cross-correlation coefficient between the electron density and the CMB to determine the best-fit parameters. This can be applied to finding gas profiles in voids or around different types of galaxies.
2. Baryon content at different redshifts. With ever increasing size and volume coverage of galaxy redshift surveys, we can create momentum templates based on galaxy surveys binned at different redshifts. We can then trace the evolution of electron density through a large redshift range.

VI. CONCLUSION

We have presented a new method of generating a template for the kinetic Sunyaev-Zel'dovich that can be used to detect the missing baryons. This momentum template is based on computing the product of a reconstructed velocity field with a galaxy field. Since the kinetic Sunyaev-Zel'dovich effect is a line of sight integral of electron momenta (modulo constants such as Thompson scattering cross-section), the combination of a galaxy redshift survey and a CMB survey can detect the ionized gas.

Unlike other techniques that look for hot gas or metals, this approach directly detects the electrons in the IGM through their signature on the CMB. Since the kSZ is produced simply by Thompson scattering from free electrons, there is no need for detailed knowledge about the metallicity of the medium and its evolution, nor for an understanding of potentially out-of-equilibrium level populations.

The kSZ amplitude is the product of the gas density and its velocity, and the latter, as we have shown, can be well-modeled by linear theory, providing an independent check, on different scales and relying on different physics, from baryon surveys that employ tracers that scale as the square of density, or that are more concentrated in the center of the most massive virialized objects.

Our studies in this paper find that a CMB survey, with sufficient resolution to push past the ‘‘damping tail’’ of

the primordial fluctuations but not necessarily covering the entire sky, partnered with an overlapping galaxy survey with sufficient number density to find structures at these angular scales, can provide an unambiguous detection of the baryons.

We have estimate the expected signal-to-noise for detecting the galaxy-momentum kSZ cross-correlation for a few different combinations of current and upcoming experiments. The estimated signal-to-noise for detecting the galaxy-momentum kSZ cross-correlation is 4.1, 8.5, 12.2 for ACT (with survey area of 2000 deg²) with SDSS-DR4, SDSS3 and ADEPT. The estimated signal-to-noise for PLANCK with SDSS-DR4, SDSS3 and ADEPT is 11.2, 22.5 and 32.2. The proposed estimator provides an exciting avenue into understanding the ionized gas in the Universe in the near future.

We have produced momentum templates from Sloan Digital Sky Survey, so that the scientific community make take arcminute scale CMB data from current and upcoming experiments such as ACT, SPT and PLANCK and determine not only the gas fraction of the Universe, but also the distribution and evolution of the gas fractions and gas profiles around different regions in the sky.

Acknowledgments

We thank Paul Bode for his help in simulations, Martin White, Jerry Ostriker, Jo Dunkley and Joe Hennawi for insightful comments. Shirley Ho and David Spergel's work on this project has been partially supported by the NASA WMAP project, NASA grant NNX08AH30G and NSF grant 0707731.

Funding for the SDSS and SDSS-II has been provided by the Alfred P. Sloan Foundation, the Participating Institutions, the National Science Foundation, the U.S. Department of Energy, the National Aeronautics and Space Administration, the Japanese Monbukagakusho, the Max Planck Society, and the Higher Education Funding Council for England. The SDSS Web Site is <http://www.sdss.org/>.

The SDSS is managed by the Astrophysical Research Consortium for the Participating Institutions. The Participating Institutions are the American Museum of Natural History, Astrophysical Institute Potsdam, University of Basel, University of Cambridge, Case Western Reserve University, University of Chicago, Drexel University, Fermilab, the Institute for Advanced Study, the Japan Participation Group, Johns Hopkins University, the Joint Institute for Nuclear Astrophysics, the Kavli Institute for Particle Astrophysics and Cosmology, the Korean Scientist Group, the Chinese Academy of Sciences (LAMOST), Los Alamos National Laboratory, the Max-Planck-Institute for Astronomy (MPIA), the Max-Planck-Institute for Astrophysics (MPA), New Mexico State University, Ohio State University, University of Pittsburgh, University of Portsmouth, Princeton University, the United States Naval Observatory, and the Uni-

versity of Washington.

-
- [1] G. Steigman, *ARNPS* **57**, 463 (2007), arXiv:0712.1100.
- [2] D. N. Spergel, R. Bean, O. Doré, M. R. Nolta, C. L. Bennett, J. Dunkley, G. Hinshaw, N. Jarosik, E. Komatsu, L. Page, et al., *ApJS* **170**, 377 (2007), arXiv:astro-ph/0603449.
- [3] M. Rauch, *ARA&A* **36**, 267 (1998), arXiv:astro-ph/9806286.
- [4] J. N. Bregman, *ARA&A* **45**, 221 (2007), arXiv:0706.1787.
- [5] W. Forman and C. Jones, *Ann. Rev. Astron. Astrophys.* **20**, 547 (1982).
- [6] C. L. Sarazin, *Reviews of Modern Physics* **58**, 1 (1986).
- [7] P. Rosati, S. Borgani, and C. Norman, *Ann. Rev. Astron. Astrophys.* **40**, 539 (2002), arXiv:astro-ph/0209035.
- [8] J. M. Shull, *Nature (London)* **433**, 465 (2005).
- [9] P. Gomez, A. K. Romer, J. B. Peterson, W. Chase, M. Runyan, W. Holzappel, C. L. Kuo, M. Newcomb, J. Ruhl, J. Goldstein, et al., in *Plasmas in the Laboratory and in the Universe: New Insights and New Challenges*, edited by G. Bertin, D. Farina, and R. Pozzoli (2004), vol. 703 of *American Institute of Physics Conference Series*, pp. 361–366.
- [10] L. Cao, J. Liu, and L.-Z. Fang, *ApJ* **661**, 641 (2007).
- [11] C. Hernández-Monteagudo and J. A. Rubiño-Martín, *MNRAS* **347**, 403 (2004), arXiv:astro-ph/0305606.
- [12] J. Dunkley, E. Komatsu, M. R. Nolta, D. N. Spergel, D. Larson, G. Hinshaw, L. Page, C. L. Bennett, B. Gold, N. Jarosik, et al., *ArXiv e-prints* **803** (2008), 0803.0586.
- [13] Z. Staniszewski, P. A. R. Ade, K. A. Aird, B. A. Benson, L. E. Bleem, J. E. Carlstrom, C. L. Chang, H. Cho, T. M. Crawford, A. T. Crites, et al., *ArXiv e-prints* (2008), 0810.1578.
- [14] R. A. Sunyaev and I. B. Zeldovich, *MNRAS* **190**, 413 (1980).
- [15] A. D. Myers, T. Shanks, P. J. Outram, W. J. Frith, and A. W. Wolfendale, *MNRAS* **347**, L67 (2004), arXiv:astro-ph/0306180.
- [16] N. Sehgal, H. Trac, K. Huffenberger, and P. Bode, *Astrophys. J.* **664**, 149 (2007), arXiv:astro-ph/0612140.
- [17] E. Komatsu and U. Seljak, *Mon. Not. R. Astron. Soc.* **336**, 1256 (2002), arXiv:astro-ph/0205468.
- [18] S. DeDeo, D. N. Spergel, and H. Trac, *ArXiv Astrophysics e-prints* (2005), arXiv:astro-ph/0511060.
- [19] O. Doré, J. F. Hennawi, and D. N. Spergel, *ApJ* **606**, 46 (2004), arXiv:astro-ph/0309337.
- [20] M. A. Strauss and J. A. Willick, *Phys. Rep.* **261**, 271 (1995), arXiv:astro-ph/9502079.
- [21] M. Tegmark, M. R. Blanton, M. A. Strauss, F. Hoyle, D. Schlegel, R. Scoccimarro, M. S. Vogele, D. H. Weinberg, I. Zehavi, A. Berlind, et al., *Astrophys. J.* **606**, 702 (2004), arXiv:astro-ph/0310725.
- [22] C. M. Springob, K. L. Masters, M. P. Haynes, R. Giovanelli, and C. Marinoni, *Astrophys. J. Supp.* **172**, 599 (2007), 0705.0647.
- [23] K. L. Masters, in *Frontiers of Astrophysics: A Celebration of NRAO's 50th Anniversary*, edited by A. H. Bridle, J. J. Condon, and G. C. Hunt (2008), vol. 395 of *Astronomical Society of the Pacific Conference Series*, pp. 137–+.
- [24] E. Bertschinger, *ApJS* **137**, 1 (2001), arXiv:astro-ph/0103301.
- [25] P. McDonald, H. Trac, and C. Contaldi, *MNRAS* **366**, 547 (2006), arXiv:astro-ph/0505565.
- [26] P. Bode and J. P. Ostriker, *ApJS* **145**, 1 (2003), arXiv:astro-ph/0302065.
- [27] M. J. I. Brown, Z. Zheng, M. White, A. Dey, B. T. Januzzi, A. J. Benson, K. Brand, M. Brodwin, and D. J. Croton, *Astrophys. J.* **682**, 937 (2008), arXiv:0804.2293.
- [28] J. P. Ostriker and E. T. Vishniac, *ApJl* **306**, L51 (1986).
- [29] A. Cooray and W. Hu, *ApJ* **534**, 533 (2000), arXiv:astro-ph/9910397.
- [30] N. Y. Gnedin and L. Hui, *MNRAS* **296**, 44 (1998), arXiv:astro-ph/9706219.
- [31] W. Hu, *Astrophys. J.* **529**, 12 (2000), arXiv:astro-ph/9907103.
- [32] M. R. Blanton, D. J. Schlegel, M. A. Strauss, J. Brinkmann, D. Finkbeiner, M. Fukugita, J. E. Gunn, D. W. Hogg, Ž. Ivezić, G. R. Knapp, et al., *Astron. J.* **129**, 2562 (2005), arXiv:astro-ph/0410166.
- [33] D. J. Eisenstein, I. Zehavi, D. W. Hogg, R. Scoccimarro, M. R. Blanton, R. C. Nichol, R. Scranton, H.-J. Seo, M. Tegmark, Z. Zheng, et al., *Astrophys. J.* **633**, 560 (2005), arXiv:astro-ph/0501171.
- [34] S. Ho, C. Hirata, N. Padmanabhan, U. Seljak, and N. Bahcall, *Phys. Rev. D* **78**, 043519 (2008).
- [35] D. K. Erb, C. C. Steidel, A. E. Shapley, M. Pettini, N. A. Reddy, and K. L. Adelberger, *Astrophys. J.* **647**, 128 (2006), arXiv:astro-ph/0604388.
- [36] D. G. York, J. Adelman, J. E. Anderson, Jr., S. F. Anderson, J. Annis, N. A. Bahcall, J. A. Bakken, R. Barkhouser, S. Bastian, E. Berman, et al., *Astron. J.* **120**, 1579 (2000), arXiv:astro-ph/0006396.
- [37] J. E. Gunn, M. Carr, C. Rockosi, M. Sekiguchi, K. Berry, B. Elms, E. de Haas, Ž. Ivezić, G. Knapp, R. Lupton, et al., *Astron. J.* **116**, 3040 (1998), arXiv:astro-ph/9809085.
- [38] J. E. Gunn, W. A. Siegmund, E. J. Mannery, R. E. Owen, C. L. Hull, R. F. Leger, L. N. Carey, G. R. Knapp, D. G. York, W. N. Boroski, et al., *Astron. J.* **131**, 2332 (2006), arXiv:astro-ph/0602326.
- [39] D. W. Hogg, M. Blanton, and SDSS Collaboration, in *Bulletin of the American Astronomical Society* (2001), vol. 34 of *Bulletin of the American Astronomical Society*, pp. 570–+.
- [40] M. Fukugita, T. Ichikawa, J. E. Gunn, M. Doi, K. Shimasaku, and D. P. Schneider, *Astron. J.* **111**, 1748 (1996).
- [41] J. A. Smith, D. L. Tucker, S. Kent, M. W. Richmond, M. Fukugita, T. Ichikawa, S.-i. Ichikawa, A. M. Jorgensen, A. Uomoto, J. E. Gunn, et al., *Astron. J.* **123**, 2121 (2002), arXiv:astro-ph/0201143.
- [42] R. Lupton, J. E. Gunn, Z. Ivezić, G. R. Knapp, and S. Kent, in *Astronomical Data Analysis Software and Systems X*, edited by F. R. Harnden, Jr., F. A. Primini, and H. E. Payne (2001), vol. 238 of *Astronomical Society of the Pacific Conference Series*, pp. 269–+.

- [43] J. R. Pier, J. A. Munn, R. B. Hindsley, G. S. Hennessy, S. M. Kent, R. H. Lupton, and Ž. Ivezić, *Astron. J.* **125**, 1559 (2003), arXiv:astro-ph/0211375.
- [44] D. L. Tucker, S. Kent, M. W. Richmond, J. Annis, J. A. Smith, S. S. Allam, C. T. Rodgers, J. L. Stute, J. K. Adelman-McCarthy, J. Brinkmann, et al., *Astronomische Nachrichten* **327**, 821 (2006), arXiv:astro-ph/0608575.
- [45] N. Padmanabhan, D. J. Schlegel, D. P. Finkbeiner, J. C. Barentine, M. R. Blanton, H. J. Brewington, J. E. Gunn, M. Harvanek, D. W. Hogg, Z. Ivezić, et al., *ArXiv Astrophysics e-prints* (2007), astro-ph/0703454.
- [46] D. J. Eisenstein, J. Annis, J. E. Gunn, A. S. Szalay, A. J. Connolly, R. C. Nichol, N. A. Bahcall, M. Bernardi, S. Burles, F. J. Castander, et al., *Astron. J.* **122**, 2267 (2001), arXiv:astro-ph/0108153.
- [47] M. A. Strauss, D. H. Weinberg, R. H. Lupton, V. K. Narayanan, J. Annis, M. Bernardi, M. Blanton, S. Burles, A. J. Connolly, J. Dalcanton, et al., *Astron. J.* **124**, 1810 (2002), arXiv:astro-ph/0206225.
- [48] G. T. Richards, X. Fan, H. J. Newberg, M. A. Strauss, D. E. Vanden Berk, D. P. Schneider, B. Yanny, A. Boucher, S. Burles, J. A. Frieman, et al., *Astron. J.* **123**, 2945 (2002), arXiv:astro-ph/0202251.
- [49] M. R. Blanton, H. Lin, R. H. Lupton, F. M. Maley, N. Young, I. Zehavi, and J. Loveday, *Astron. J.* **125**, 2276 (2003), arXiv:astro-ph/0105535.
- [50] C. Stoughton, J. Adelman, J. T. Annis, J. Hendry, J. Inkmann, S. Jester, S. M. Kent, N. Kuropatkin, B. Lee, H. Lin, et al., in *Society of Photo-Optical Instrumentation Engineers (SPIE) Conference Series*, edited by J. A. Tyson and S. Wolff (2002), vol. 4836 of *Presented at the Society of Photo-Optical Instrumentation Engineers (SPIE) Conference*, pp. 339–349.
- [51] K. Abazajian, J. K. Adelman-McCarthy, M. A. Agüeros, S. S. Allam, S. F. Anderson, J. Annis, N. A. Bahcall, I. K. Baldry, S. Bastian, A. Berlind, et al., *Astron. J.* **126**, 2081 (2003).
- [52] K. Abazajian, J. K. Adelman-McCarthy, M. A. Agüeros, S. S. Allam, K. Anderson, S. F. Anderson, J. Annis, N. A. Bahcall, I. K. Baldry, S. Bastian, et al., *Astron. J.* **128**, 502 (2004), arXiv:astro-ph/0403325.
- [53] K. Abazajian, J. K. Adelman-McCarthy, M. A. Agüeros, S. S. Allam, K. S. J. Anderson, S. F. Anderson, J. Annis, N. A. Bahcall, I. K. Baldry, S. Bastian, et al., *Astron. J.* **129**, 1755 (2005), arXiv:astro-ph/0410239.
- [54] J. K. Adelman-McCarthy and et al., *VizieR Online Data Catalog* **2276**, 0 (2007).
- [55] J. K. Adelman-McCarthy, M. A. Agüeros, S. S. Allam, K. S. J. Anderson, S. F. Anderson, J. Annis, N. A. Bahcall, C. A. L. Bailer-Jones, I. K. Baldry, J. C. Barentine, et al., *Astrophys. J Supp.* **172**, 634 (2007), arXiv:0707.3380.
- [56] J. K. Adelman-McCarthy and for the SDSS Collaboration, *ArXiv e-prints* **707** (2007), 0707.3413.
- [57] R. K. Sachs and A. M. Wolfe, *Astrophys. J.* **147**, 73 (1967).
- [58] M. J. Rees and D. W. Sciama, *Nature (London)* **217**, 511 (1968).
- [59] A. W. Blain, in *Deep Fields*, edited by S. Cristiani, A. Renzini, and R. E. Williams (2001), pp. 129–+.
- [60] D. J. Schlegel, D. P. Finkbeiner, and M. Davis, *Astrophys. J.* **500**, 525 (1998), arXiv:astro-ph/9710327.
- [61] Available at <http://arcturus.mit.edu/grafic/>
- [62] Available at <http://www.astro.princeton.edu/~bode/TPM/>
- [63] <http://www.physics.princeton.edu/act/>
- [64] <http://www.rssd.esa.int/index.php?project=Planck>
- [65] <http://www.sdss3.org>
- [66] <http://universe.nasa.gov/program/probes/adept.html>
- [67] <http://www.astro.princeton.edu/~shirley/SZ/SZ.html>